Annals of Botany **107**: 1235–1245, 2011
doi:10.1093/aob/mcq247, available online at www.aob.oxfordjournals.org

ANNALS OF BOTANY
Founded 1887

PART OF A SPECIAL ISSUE ON THE PLANT CELL CYCLE

Spatial and temporal profiles of cytokinin biosynthesis and accumulation in developing caryopses of maize

Tomaž Rijavec[1,‡], Mukesh Jain[2], Marina Dermastia[1,*] and Prem S. Chourey[3,4]

[1]*National Institute of Biology, Večna pot 111, 1000 Ljubljana, Slovenia,* [2]*Agronomy Department, University of Florida, Gainesville, FL 32611-0680, USA,* [3]*United States Department of Agriculture-Agricultural Research Service, Center for Medical, Agricultural, and Veterinary Entomology, Chemistry Unit, Gainesville, FL 32608-1069, USA and* [4]*Agronomy and Plant Pathology Departments, University of Florida, Gainesville, FL 32611-0680, USA*
[‡]*Present address: Institute for Physical Biology, Toplarniška 19, 1000 Ljubljana, Slovenia*
* *For correspondence. E-mail marina.dermastia@nib.si*

Received: 5 July 2010 Returned for revision: 24 August 2010 Accepted: 2 November 2010 Published electronically: 17 December 2010

• *Background and Aims* Cytokinins are a major group of plant hormones and are associated with various developmental processes. Developing caryopses of maize have high levels of cytokinins, but little is known about their spatial and temporal distribution. The localization and quantification of cytokinins was investigated in maize (*Zea mays*) caryopsis from 0 to 28 d after pollination together with the expression and localization of isopentenyltransferase ZmIPT1 involved in cytokinin biosynthesis and *ZmCNGT*, the gene putatively involved in *N*9-glucosylation.
• *Methods* Biochemical, cellular and molecular approaches resolved the overall cytokinin profiles, and several gene expression assays were used for two critical genes to assess cytokinin cell-specific biosynthesis and conversion to the biologically inactive form. Cytokinins were immunolocalized for the first time in maize caryopses.
• *Key Results* During the period 0–28 d after pollination (DAP): (1) large quantities of cytokinins were detected in the maternal pedicel region relative to the filial tissues during the early stages after fertilization; (2) unpollinated ovules did not accumulate cytokinins; (3) the maternal nucellar region showed little or no cytokinin signal; (4) the highest cytokinin concentrations in filial endosperm and embryo were detected at 12 DAP, predominantly zeatin riboside and zeatin-9-glucoside, respectively; and (5) a strong cytokinin immuno-signal was detected in specific cell types in the pedicel, endosperm and embryo.
• *Conclusions* The cytokinins of developing maize caryopsis may originate from both local syntheses as well as by transport. High levels of fertilization-dependent cytokinins in the pedicel suggest filial control on metabolism in the maternal tissue; they may also trigger developmental programmed cell death in the pedicel.

Key words: Caryopsis, cytokinins, immunolocalization, maize, *N*9-glucosylation, programmed cell death, *Zea mays*.

INTRODUCTION

Initiation of normal development of a maize one-seeded fruit caryopsis depends on the successful completion of pollination and fertilization. At maturity, the caryopsis consists of a pericarp and a highly structured embryo surrounded by a copious nutritive endosperm, which constitutes the bulk of the caryopsis. At the base of the endosperm is an endosperm transfer layer (BETL), which provides the primary interface between maternal and filial tissues in the developing maize caryopsis (Kang *et al.*, 2009). The pedicel is the major structural bridge in the transfer of photosynthates and nutrients from the maternal plant to the developing caryopsis. Within the pedicel, immediately below the BETL, are placento-chalazal (P-C) cells. The P-C layer is thought to have a critical role in the post-vascular transport of water, sugars and nutrients for developing seeds (Kladnik *et al.*, 2004). The maize P-C layer is also presumed to function in the antimicrobial protection of the developing seed through the accumulation of phenolic compounds (Kladnik *et al.*, 2004; LeClere *et al.*, 2007). Programmed cell death (PCD) occurs in two spatially and temporally distinctive sub-domains, which coincide with nucellar and integumental P-C layers based on their developmental origins. Moreover, the early phase of PCD is specific only to the fertilized caryopses (Kladnik *et al.*, 2004).

Generally, most or all of the normal fruit developmental programmes depend on the spatial and temporal synthesis and action of plant hormones. The extremely high concentrations of cytokinins (CKs) and a number of expressed CK metabolic enzymes in the maize caryopsis indicate their possible association with the development of caryopsis (Jones *et al.*, 1990; Lur and Setter, 1993; Dietrich *et al.*, 1995; Brugière *et al.*, 2003; Veach *et al.*, 2003; Rijavec *et al.*, 2009). Despite intensive study, it remains largely unknown if the huge amount of CKs detected in maize caryopsis is a consequence of their transport from the maternal tissues to the filial tissues or *de novo* biosynthesis of CKs within the seed itself. In addition, data on specific CK localization within the caryopsis are scarce and to the best of our knowledge there is no report on maize caryopsis CK immunolocalization. However, CKs are generally considered as promoters of cell division, and their high transient abundance in caryopsis

occurs between 6 and 10 d after pollination (DAP) (Dietrich *et al.*, 1995; Brugière *et al.*, 2003; Rijavec *et al.*, 2009) with a peak of endosperm mitotic index at 12 DAP (reviewed in Morris, 1997). This type of observation has led to hypotheses in which the main role of caryopsis CKs is establishing maize seed size by promoting cell divisions in the endosperm or increasing the sink strength of seeds for assimilates. Nevertheless, caryopsis CKs may have other physiological roles (Brugière *et al.*, 2008; Rijavec *et al.*, 2009).

Several recent studies in maize show the expression of different CK biosynthetic genes encoding ATP/ADP isopentenyltransferases (IPTs) in developing caryopses. The IPT genes *ZmIPT1*, *ZmIPT2* and *ZmIPT10* are expressed in the pedicel, endosperm and embryo (Brugière *et al.*, 2008; Šmehilová *et al.*, 2009; Vyroubalová *et al.*, 2009). *ZmIPT2* expression in the BETL, 8 DAP, coincides with a high level of ZmIPT2 protein in the same region (Brugière *et al.*, 2008). The expression of *ZmIPT* coincides with accumulation of *trans*-zeatin riboside (ZR) (Brugière *et al.*, 2008) and other CK metabolites in maize caryopsis, especially in its basal section (Rijavec *et al.*, 2009).

Degradation or reversible/irreversible inactivation are key regulators of CK levels. For example, several maize CK dehydrogenase (*CKX*s) genes are expressed in the caryopsis pedicel region, endosperm and embryo (Massonneau *et al.*, 2004; Šmehilová *et al.*, 2009; Vyroubalová *et al.*, 2009) and their corresponding proteins irreversibly cleave the N^6-side chain from the main purine ring (Massonneau *et al.*, 2004). Recently, increased levels of zeatin-*O*-glucoside have been reported in roots and leaves of maize transformants harbouring the *ZOG1* gene encoding a zeatin-*O*-glucosyltransferase from *Phaseolus lunatus* (Rodó *et al.*, 2008). In non-transformed maize, *cis*-zeatin riboside-*O*-glucoside was a major CK metabolite in caryopsis (Veach *et al.*, 2003). Although the exact role of CK-*O*-glucosides is not clear, they are generally assumed to be storage products (Martin *et al.*, 2001). Information on the molecular biology of CK-*N*-glucosides, a group of metabolically inactive CKs (Brzobohatý *et al.*, 1994), is scarce (Hou *et al.*, 2004) and currently unavailable for maize. However, in maize caryopsis there is a notably high concentration of *trans*-zeatin-9-glucoside (Z9G) recorded in the developmental phase 10 DAP following intense mitotic activity (Veach *et al.*, 2003; Rijavec *et al.*, 2009).

The aim of the present study was to investigate: (1) the distribution of CKs in developing maize caryopsis by immunolocalization, used here for the first time in caryopsis; (2) the expression and localization of *ZmIPT1* involved in CK biosynthesis; and (3) the expression and localization of *ZmCNGT*, the gene putatively involved in *N*9-glucosylation, to shed light on this irreversible CK inactivation during caryopsis development. We hypothesize that *de novo* synthesis in caryopsis and/or CK transport from the maternal plant are associated with the pollination event and that the high CK concentration in the basal part of the caryopsis is associated with the development of the P-C layer in the pedicel.

MATERIALS AND METHODS

Plant material

Maize (*Zea mays* L.) plants of the W22 inbred line were grown in greenhouses and in experimental fields at the University of Florida, Gainesville, USA, and at the National Institute of Biology, Ljubljana, Slovenia, during the summers of 2006, 2007 and 2008. Cobs from non-pollinated and hand-pollinated plants were collected at 0, 6, 8, 10, 12, 16, 20 and 28 DAP and were transported to the lab on ice. Individual unfertilized ovules and developing caryopses were frozen in liquid nitrogen immediately after excision and stored at −80 °C. Frozen plant material used for biochemical analysis of CK content was lyophilized at −60 °C and stored in a desiccator. Embryos (at 12, 16, 20 and 28 DAP developmental stages) and endosperm tissue (at 8, 12, 16, 20 and 28 DAP developmental stages) were used for isolation of RNA from fresh caryopses, while for CK biochemical analysis they were collected from lyophilized caryopses.

Immunolocalization of CKs

Fresh intact caryopses were cut on both sides to allow the solutions and fixatives to penetrate into the tissue. In order to cross-link cellular proteins with CK ribosides and glycosides, potentially present in caryopsis, reactions for preparing protein conjugates with any glycosides possessing neighbouring hydroxyl groups (Erlanger and Beiser, 1964) adopted for immunolocalization studies of CKs (Sossountzov *et al.*, 1988) were performed. The reactions were applied prior to paraformaldehyde–glutaraldehyde tissue fixation, which binds only CK bases to cellular proteins (Dewitte *et al.*, 1999). In brief, plant samples were incubated in freshly prepared 20 mM sodium periodate (Sigma, St Louis, MO, USA) in 50 mM carbonate–bicarbonate buffer, pH 9·6, in a vacuum at room temperature for 2 h. The solution was renewed every 30 min. Samples were transferred to freshly prepared 2 mM $NaBH_4$ (Sigma) in 70 mM Tris buffer, pH 7·6, and incubated in a vacuum at room temperature for 1 h. Plant material was then fixed under vacuum using 4 % paraformaldehyde (Agar Scientific, Stansted, UK) and 0·1 % glutaraldehyde (Merck KGaA, Darmstadt, Germany) in half-strength PBS, pH 7·6, at room temperature for 6 h. Samples were dehydrated in an ethanol series (100, 90, 70, 50 and 30 %, H_2O), embedded in Paraplast Plus (Fisher Scientific, Loughborough, UK) and sectioned (12 μm) on a rotary microtome (Microm 325; Carl Zeiss, Jena, Germany). The sections were fixed onto glass slides at 40 °C.

All immunostaining treatments were carried out at room temperature. Tissue sections were de-waxed and covered with blocking buffer [100 mM PBS, 0·5 % (w/v) bovine serum albumin, 1 % (v/v) normal goat serum, 20 mM glycine] and washed with wash buffer [100 mM PBS, 0·025 % (v/v) Tween 20]. Rabbit primary antibodies raised against ZR were obtained from OlChemim Ltd (Olomouc, Czech Republic). According to the manufacturer's specification, the antibodies cross-reacted with other CKs as follows: *trans*-ZR, 100 %; *trans*-zeatin (Z), 37 %; *trans*-Z9G, 93·5 %; dihydrozeatin riboside (DHZR), 2·36 %; dihydrozeatin (DHZ), 1·52 %; isopentenyladenosine (iPA), 1·39 %; isopentenyladenine (iP), 0·87 %. The cross-reactivity with *O*-glucosides is not reported. Concentrations of 3·5 ng μL^{-1} were used for the primary antibody binding. Sheep anti-rabbit secondary antibody labelled with alkaline phosphatase (AP) (Jackson Immunoresearch Laboratories, Inc., Pennsylvania, PA, USA) was used at a dilution of 1 :

1000. Unbound secondary antibodies were washed off with 0·025 % Tween 20 in PBS. AP substrate buffer (100 mM NaCl, 100 mM Tris–HCl, pH 9·5) was applied, followed by NBT/BCIP AP substrate (Roche, Mannheim, Germany) diluted to 1 : 50 in AP substrate buffer. AP reaction was carried out between 30 min to 1 h in darkness and the solutions were washed off with water. The reaction was visualized using an Axioskop 2 MOT microscope (Carl Zeiss) and an AxioCam MRc digital colour camera (Carl Zeiss Vision, Hallbergmoos, Germany).

The following stringent controls for the immunolocalization method were processed in parallel in every experiment on adjacent sections in treatments (1) without primary or (2) secondary antibodies; (3) with an excess of synthetic ZR, Z, Z9G, DHZR and iPA in five-fold higher concentrations as those of the antibodies to ensure their saturation; (4) with concentrated pre-immune rabbit serum; (5) with diluted serum; (6) with omission of the coupling step between cellular proteins, ribosides and glucosides; and (7) with the methanol wash of fixed tissue sections with no cross-linking of CKs and cellular proteins.

Biochemical analysis of CKs

Quantification of the most abundant CK metabolites in maize caryopsis was performed essentially as described by Rijavec *et al.* (2009). Briefly, CKs were extracted in 80 % ice-cold methanol and partially cleaned of impurities by ion-exchange chromatography using polyvinylpolypirolidone (Sigma) from lyophilized caryopsis harvested at different DAP. CKs were further purified and concentrated by immunoaffinity chromatography using isoprenoid CK antibodies (OlChemim Ltd) and analysed by high-performance liquid chromatography (HPLC) using a Nova Pack C18 column (4-μm spherical particles, 150 mm × 3·9 mm; Waters, Milford, MA, USA) and a Waters 996 photodiode array spectrophotometer (Waters). CK metabolites were identified on the basis of retention times and spectral properties of a set of standards: Z, ZR, Z9G, DHZR, DHZ, dihydrozeatin-9-glucoside (DHZ9G), iP, iPA and isopentenyladeneine-9-glucoside (iP9G) (all from OlChemim). CKs in samples were quantified by integrating the areas under the peaks measured at 265 nm and comparing them with integrated areas of peaks of known standard quantities. The efficiency of the isolation method was estimated by running known quantities of standards through the extraction, isolation and quantification procedure, either alone or added to the sample. Recoveries for each isoprenoid CK species were as follows: Z, 38–40 %; DHZ, 30–36 %; iP, 2–4 %; ZR, 58–59 %; DHZR, 52–56 %; iPA, 22–24 %; Z9G, 59–61 %; DHZ9G, 45–50 %; iP9G, 24–28 %. The data obtained were normalized accordingly.

Expression analysis of the putative ZmCNGT *gene*

The gene sequence for *N*-glucosyl transferase denoted here as *ZmCNGT* was retrieved by database expressed sequence tag (EST) searches, using TBLASTN at NCBI (http://www.ncbi.nlm.nih.gov/BLAST/). Known *Arabidopsis* CNGT protein sequences (UGT76C1 – GI: 42567677 and UGT76C2 – GI: 42567678) (Hou *et al.*, 2004) were used as probes. Unidentified maize candidate EST sequences were assembled to obtain a full length transcript, were further translated to protein using the Expasy Translate tool (http://expasy.org/tools/dna.html) and aligned with *Arabidopsis* glucosyl transferase protein sequences, using the Clustal align algorithm (Chenna *et al.*, 2003). Similarity was cross-checked with the EMBOSS Pairwise Alignment Algorithm Needle (http://www.ebi.ac.uk/emboss/align/) using default gap penalties and EBLOSSUM62 as the substitution matrix (Supplementary Data Fig. S1, available online).

For RNA isolation, about 2 g of frozen caryopsis material was ground in liquid N_2. RNA was isolated using the LiCl and acidic phenol isolation method (Sambrook *et al.*, 1989). RNA was quantified using the NanoDrop™ spectrophotometer (Thermo Scientific, Wilmington, DE, USA) and checked for quality using a native 1 % agarose gel. Five micrograms of total RNA was reverse transcribed using the SuperScript® III First-strand Synthesis System (Invitrogen, Carlsbad, CA, USA) according to the manufacturer's protocol. A quantitative real-time PCR was performed using the Dynamo™ HS SYBR® Green qPCR Kit (Finnzymes, Espoo, Finland) and Chromo 4™ CFD (MJ Research, Alameda, CA, USA) supported by Opticon Monitor™ Software version 2·03 (MJ Research). A 157-bp amplicon was amplified using the primer pair 5′AGCAGATAGTGAACGCGAGGTATGTG3′ and 5′TTAAGAAGCCGAGCCCTCTCCCTT3′. The thermal cycling protocol entailed incubation at 50 °C for 2 min, followed by *Tbr* DNA polymerase activation at 95 °C for 15 min. PCR amplification was carried out for 35 cycles with denaturation at 94 °C for 10 s, and primer annealing and extension at 55 and 72 °C, respectively, for 30 s each. Optical data were acquired following the extension step, and the PCR reactions were subjected to melting curve analysis beginning at 55 °C through to 95 °C, at 1 °C s^{-1}. Three independently made reverse transcriptase preparations (from two separate RNA isolations) were used for transcript quantification each in three replicate real-time PCR reactions. Absolute quantification of gene transcripts was performed according to Whelan *et al.* (2003). A 946-bp gene fragment was PCR-amplified using gene-specific primers 5′ATCAAA GAAGAGCGGCTGGACGA3′ and 5′CAGAGCGTCATCGT CATGCTGAA3′. The thermal cycling protocol entailed activation of PlatinumTaq DNA polymerase (Invitrogen) at 94 °C for 5 min, followed by 35 cycles of denaturation at 94 °C and primer annealing at 55 °C for 15 s and extension at 72 °C for 1 min. The amplification reactions were finally extended for 10 min at 72 °C and held at 4 °C. The fragment was ligated into pCR4-TOPO vector (Invitrogen), sequenced and used for the standard curve.

Western blot analysis

For protein extraction, the frozen caryopses were thoroughly ground in liquid N_2. The resulting powder was suspended in extraction buffer (50 mM Tris-HCl, pH 7; 1 mM dithiothreitol; 1 mM phenylmethylsulfonyl fluoride). After centrifugation (18 000 g, 10 min at 4 °C), the supernatant was collected as the protein extract. Protein samples were immediately denatured in 2× SDS–PAGE sample buffer [0·125 M Tris-HCl; 4 % (w/v) SDS; 20 % (v/v) glycerol; 0·02 % (w/v)

bromophenol blue; pH 6·8) by boiling at 100 °C for 5 min. SDS–PAGE analyses were carried out using 8 % Pierce Presice™ Protein gel (Pierce, Rockford, IL, USA) for 1 h at 100 V. Protein blotting to polyvinylidene fluoride membrane (Immobilon-P; Millipore, Billerica, MA, USA) was performed in the BioRad Mini Trans-Blot apparatus following the manufacturer's instructions. The rabbit primary IgG anti-ZmCNGT antiserum was used at a dilution of 1 : 200 in TBS buffer (20 mM Tris, 0·5 M NaCl, pH 7·5). Antibodies were washed in TBST buffer [1 × TBS, 0·05 % (v/v) Tween 20]. The anti-mouse horseradish peroxidase (HRP)-labelled secondary antiserum (Sigma) was used at 1 : 5000 in TBS buffer. HRP signal was detected using an enhanced chemiluminescence kit (Pico; Pierce) and X-ray film.

In situ *hybridization of* ZmCNGT *and* ZmIPT1 *transcripts*

Sense and antisense digoxigenin (DIG)-labelled *ZmCNGT* and *ZmIPT1* (GenBank accession numbers FJ748891 and EU879927, respectively) RNA probes were synthesized using a DIG RNA Labeling Kit (Roche Diagnostics) from a DNA template (964 and 701 bp, respectively) cloned in pCR4-TOPO sequencing vector (Invitrogen). Developing caryopses of maize were harvested and immediately fixed in cold formalin acetic alcohol (3·7 % formaldehyde, 5 % acetic acid and 50 % ethanol) for 24 h, followed by dehydration in a series of ethanol and tertiary butyl alcohol and infiltration and embedding in Paraplast Plus paraffin (Sherwood Medical Co., St Louis, MO, USA). Paraffin-embedded 12-μm caryopsis sections were cut with a rotary microtome (Microm 325; Carl Zeiss, Walldorf, Germany). For detection of transcripts *in situ*, the sections were pre-treated, hybridized, washed and developed according to Jackson (1991). Anti-DIG primary antibody and AP-labelled secondary antibodies (Jackson Immunoresearch Laboratories) were used according to the manufacturer's recommendations. *In situ* hybridization signal was developed using NBT/BCIP (Roche) as AP substrate, resulting in a dark blue–purple reaction product.

RESULTS

CK immunolocalization control experiments

In parallel with each experiment, several immunolocalization controls were processed to confirm the specificity of the signal obtained (Fig. 1). Without a complete procedure, the control sections did not show any specific CK signal, indicating that the colour reaction was dependent on the presence of both the primary and the secondary antibodies (Fig. 1B, C). Use of the concentrated pre-immune rabbit serum showed unspecific signal (Fig. 1I), while diluted serum resulted in the absence of any signal (Fig. 1J). Without the cross-linking of CKs and cellular proteins the signal was reduced (Fig. 1K), probably due to the partial removal of ribosides and glucosides, which were not bound with the cellular proteins by the applied paraformaldehyde–glutaraldehyde tissue fixation. The methanol washing of sections on which the cross-linking procedure was not performed resulted in almost complete loss of the immuno-signal (Fig. 1L). Note that CKs are methanol-soluble. Because the antibodies raised against ZR and used herein cross-react with other CKs, especially with Z9G (for details, see Materials and methods), the immuno-signal obtained was not ZR-specific. Instead, the results represented a cumulative CK signal. However, we may deduce from the results of previous studies and from the quantitative analysis of CKs in this work, which CKs were immunolabelled following the immunolocalization process. The data agree well with reported cross-reactivity of applied antibodies with other CKs, and also with biochemical analyses. For instance, at 12 DAP the addition of synthetic ZR (Fig. 1D), which cross-reacts 100 % with antibodies, drastically reduced immunostaining in the P-C layer, while the addition of an excess of Z9G had little effect (Fig. 1F), although it cross-reacts similarly with the antibodies used. In agreement with this, at 12 DAP in the lower part of the caryopsis the amount of ZR has been reported to be high, and that of Z9G very low (Rijavec *et al.*, 2009). By contrast, Z9G prevailed in the embryo at 12 DAP (this study), and hence the embryo signal was greatly attenuated by the addition of synthetic Z9G (Fig. 1N).

CK immunolocalization in pedicel, pericarp and endosperm

Figure 2 depicts spatial profiles of CK distribution based on polyclonal anti-ZR antibodies referred to here as anti-CK, in developing caryopsis including the pedicel, basal and upper parts of endosperm, and pericarp from 0 to 8 DAP. Relative to the control, in the unfertilized ovule at 0 DAP a weak CK immuno-signal was detected only in the pedicel region (Fig. 2A) and in certain regions of the maternal nucellar region and pericarp (Fig. 2C). The highest immuno-signal during the early stages of development was seen at 6 DAP (Fig. 2E, G), most notably in the pedicel, especially in the integumental part of the P-C layer facing the pedicel (Fig. 2E) and the vasculature tissue (Fig. 2E, M, O). Notably, throughout the examined periods there was no immune-signal in the nucellar P-C layer facing the BETL (Figs 2E, I and 3A, E, I). At 6 DAP, the presence of CK was also confirmed in developing endosperm, especially in the BETL (Fig. 2E, I). Interestingly, taking into account the faint signal detected in unpollinated ovules at 0 DAP, the massive increase in the signal intensity in these maternal tissues at 6 DAP was highly dependent on pollination and fertilization. Although the distribution of immuno-signal was similar at 6 and 8 DAP, the pedicel signal was slightly weaker at 8 DAP, but still strong in the BETL (Fig. 2I).

During the later stages (Fig. 3), 12–20 DAP, the highest signal was seen at 12 DAP in the P-C layer, especially in several cell layers identified as the integumental P-C layer adjacent to a region composed of empty cells (Fig. 3A) due to developmental PCD described previously (Kladnik *et al.*, 2004). The P-C layer showed a gradual reduction in signal intensity at 16 (Fig. 3E) and 20 DAP (Fig. 3I) relative to at 12 DAP. In the filial endosperm, the BETL region appeared to show a significant level of signal relative to the control (Fig. 3A, E, I). The upper part of the caryopsis showed the highest signal in the aleurone layer and a few layers beneath in the starchy endosperm (Fig. 3C, G, K).

CK immunolocalization in embryo

Figure 4 depicts the immuno-signal in the developing embryo from 8 to 20 DAP. At 8 DAP, a very strong CK

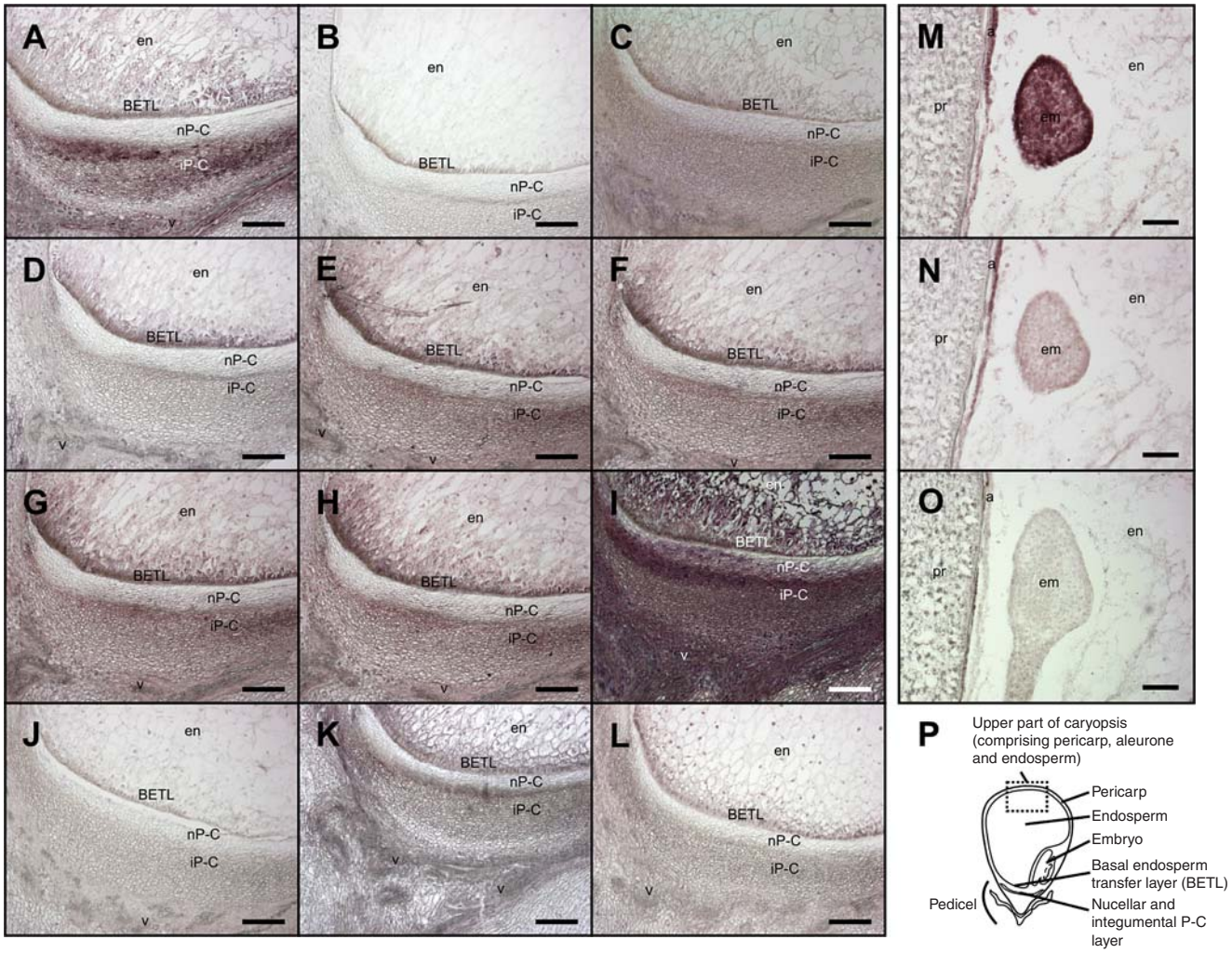

FIG. 1. Controls for CK immunolocalization reaction specificity shown on the central longitudinal section of the pedicel and lower endosperm region of developing caryopsis (A–L) and embryo (M–O) at 12 DAP. (A) Positive reaction; (B) reaction without primary antibody; (C) reaction without secondary antibody; (D) signal attenuated with the addition of an excess of synthetic ZR; (E) signal attenuated with the addition of an excess of synthetic Z; (F) signal attenuated with the addition of an excess of synthetic Z9G; (G) signal attenuated with the addition of an excess of synthetic DHZR; (H) signal attenuated with the addition of an excess of synthetic iPA; (I) treatment with pre-immune rabbit serum at 1 : 500; (J) treatment with pre-immune rabbit serum at 1 : 500 000; (K) omission of the coupling step between cellular proteins, ribosides and glucosides; (L) methanol wash of fixed tissue sections with no cross-linking of CKs and cellular proteins; (M) positive reaction; (N) signal attenuated with the addition of an excess of synthetic Z9G; (O) reaction without primary antibody; (P) schematic drawing of the caryopsis. The area visible in the panels is represented in the schematic caryopsis drawing. Abbreviations: a, aleurone; em, embryo; en, endosperm; pr, pericarp. Scale bars = 100 μm.

signal was detected in the embryo-surrounding region (ESR) of the endosperm (Fig. 4A). Although distinctive domains were not detectable at 8 DAP, there was greater staining intensity in the adaxial side than abaxial region at the globular stage of embryo development (Fig. 4A). At 12 DAP, markedly higher levels of CK were seen in root and shoot apical meristems than in suspensor and scutellar cells (Fig. 4C). Pericarp adjoining the embryo also at 12 DAP showed a positive signal (Fig. 4C). At 16 and 20 DAP, there was a CK signal in the scutellum but the highest signal level was clearly manifested in root and shoot meristematic zones (Fig. 4E, G).

Biochemical analysis of various CK forms

Figure 5 quantifies eight CK forms based on immuno-affinity chromatography and by HPLC analysis of unpollinated ovules and caryopses at 0–8 DAP, and endosperm and embryo at 12–28 DAP. Several important observations are noteworthy: caryopses comprising maternal pedicel and nucellar, and filial tissues showed 60-fold increases in CK levels relative to the unpollinated ovules. The two main metabolites in caryopses at 6 and 8 DAP were Z and ZR; these caryopses also showed the highest levels of DHZR compared with other stages. Notably, iP was detectable only in caryopses at 8 DAP, but the precise cellular location of this metabolite is not known. At 12 DAP, the first stage at which it was possible to separate endosperm and embryo for the chemical analyses, the two tissues showed a marked contrast in their levels of ZR and Z9G (Fig. 5). Whereas ZR was the most abundant CK in endosperm, in embryo it was detected only at trace levels and Z9G was predominant (Fig. 5). Additionally, although the total CK level in embryo

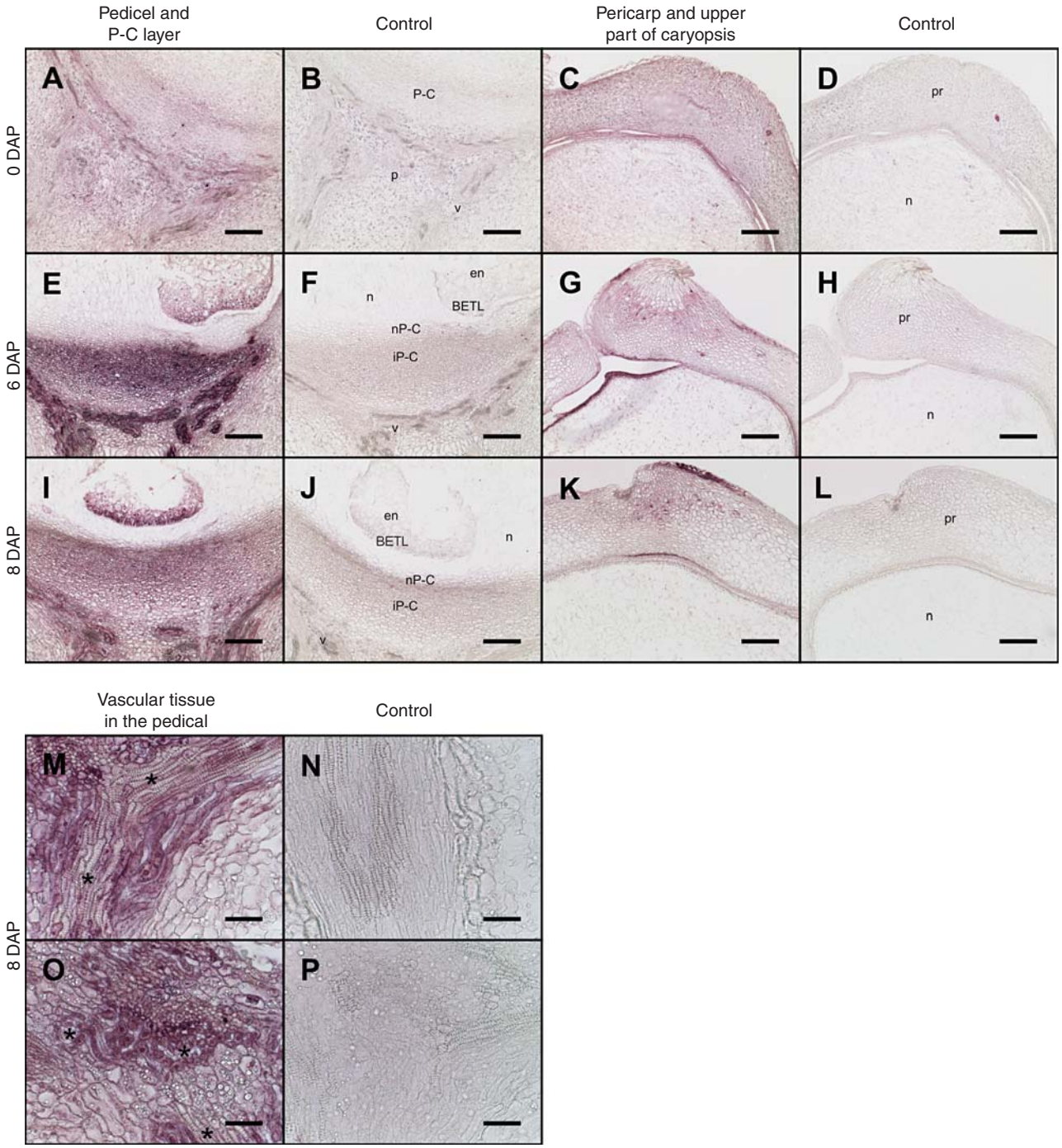

FIG. 2. CK immunolocalization on the central longitudinal section of developing maize caryopsis between 0 and 8 DAP. (A–L) Lower and upper part of caryopsis; (M–P) details of the vascular tissue in the pedicel; asterisks indicate xylem vessels. The visible area of the panels is represented in the schematic caryopsis drawing of Fig.1. Abbreviations: a, aleurone; BETL, basal endosperm transfer layer; em, embryo; en, endosperm; n, nucellus; p, pedicel; pr, pericarp; P-C, placento-chalaza; nP-C, nucellar P-C layer; iP-C, integumental P-C layer; v, vascular tissue. Scale bars (a) = 100 μm; (b) = 50 μm.

at 12 DAP was the highest of all the subsequent stages, it was only at approx. 30 % of that relative to the endosperm.

In situ *localization of* ZmIPT1 *and* ZmCNGT *transcripts*

Several lines of evidence suggest that IPT controls local CK levels by catalysing the rate-limiting step in the biosynthetic pathway of CK biosynthesis (reviewed in Hirose *et al.*, 2008). To test if there was any local CK biosynthesis in the pedicel, we carried out *in situ* hybridization analyses of the CK biosynthetic gene *ZmIPT1* at 7 and 14 DAP. The *ZmIPT1* transcript was spatially restricted to cells surrounding the vascular tissue (Fig. 6A, B), consistent with immunolocalization of CK in the pedicel region of developing maize

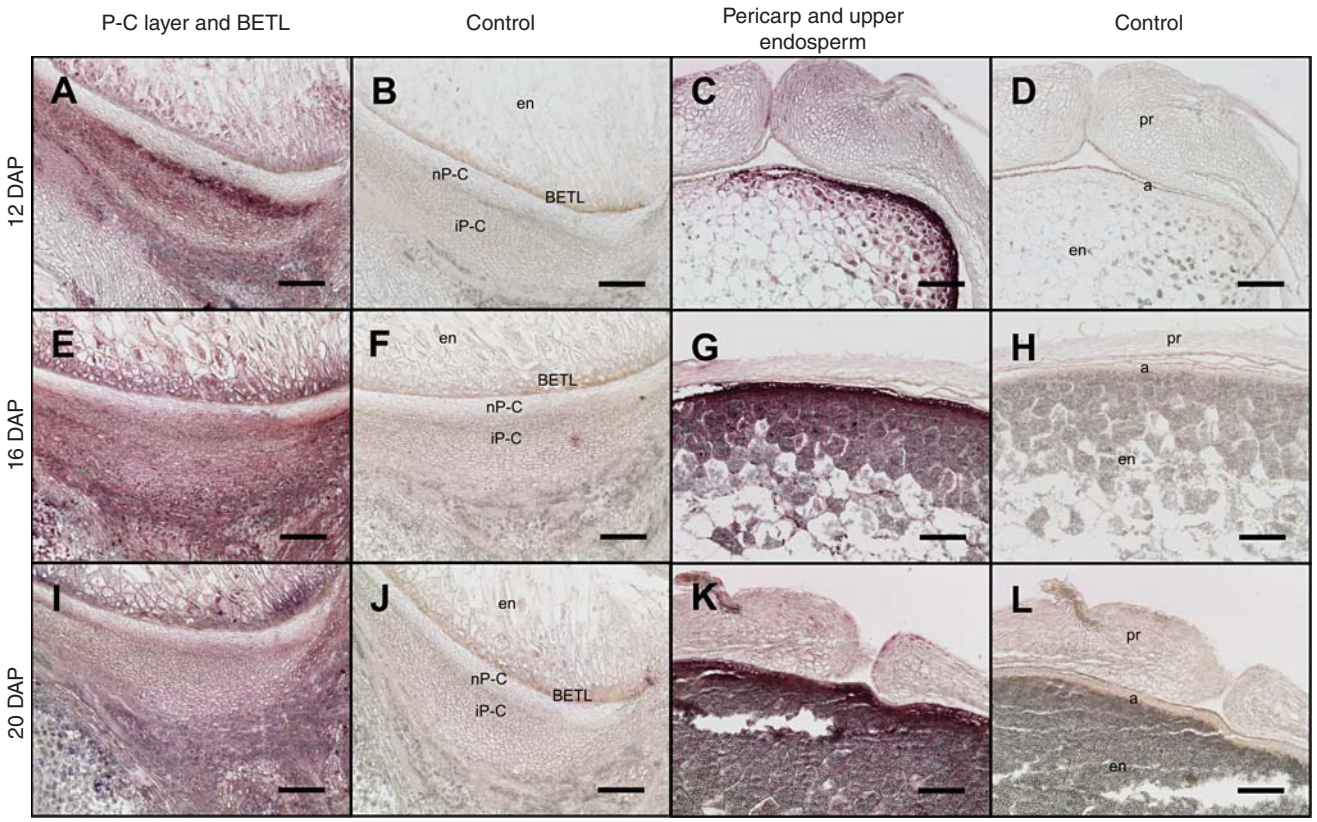

FIG. 3. CK immunolocalization on the central longitudinal section of the lower and upper part of developing maize caryopsis between 12 and 20 DAP. The area visible in the panels is represented in the schematic caryopsis drawing of Fig.1P. Abbreviations: a, aleurone; BETL, basal endosperm transfer layer; em, embryo; en, endosperm; n, nucellus; p, pedicel; pr, pericarp; P-C, placento-chalaza; nP-C, nucellar P-C layer; iP-C, integumental P-C layer; v, vascular tissue. Scale bars = 100 μm.

caryopsis (Figs 2 and 3). Likewise, *ZmCNGT* transcript was also readily localized in the pericarp (Fig. 7A, B), scutellum (Fig. 7B) and pedicel region (Fig. 7C).

Expression profiles of ZmCNGT *and the amount of Z9G during caryopsis development*

We isolated and characterized a previously unidentified putative CK *N*-glucosyl transferase gene, designated here as *ZmCNGT* (Supplementary Data Figs S1 and S2, available online), which is associated with the high *N*9-glucosylation of CK metabolites in different parts of the developing caryopsis. The expression profile of the *ZmCNGT* gene in a whole caryopsis showed a steep increase of the transcript from 0 to 8 DAP, peaking between 8 and 10 DAP and decreasing thereafter. The baseline level was reached at 28 DAP (Fig. 8A). The abundance of ZmCNGT protein (Fig. 8B) was concordant with its transcript level. Highest protein levels were observed at 12 DAP, and stayed elevated until 20 DAP; levels were reduced by 28 DAP. By contrast, quantification of a putative product of the *N*-transferase reaction, Z9G, showed its continuous increase from 6 to 28 DAP (Fig. 8A). At 28 DAP, which was the last stage examined here, 88 % of all detected CKs in the caryopsis were in the form of Z9G (data not shown).

DISCUSSION

CKs in the pedicel and their possible roles

The combined use of biochemical analysis for various CK metabolites and immunolocalization of total CK on tissue sections have led us to some novel and major insights on the spatial and temporal distribution of this hormone in ovules and developing caryopses of maize. Notably, the maternal pedicel region showed extremely high levels of CK in both the vascular tissue and the P-C layer at 6 DAP. Although these data are in agreement with previously reported biochemical data (Brugière *et al.*, 2003; Rijavec *et al.*, 2009), it was hitherto unknown whether such high CK levels were localized in the pedicel, nucellar tissue or lower part of the endosperm. Our data provide the first direct evidence of CK localization in the vascular tissue in the pedicel, and support an earlier hypothesis (Emery and Atkins, 2006) that the hormone may be transported from the mother plant to a developing seed. CKs are well recognized as a group of mobile phytohormones in plants, and their translocation and compartmentalization are greatly influenced by nutritional signalling (reviewed in Hirose *et al.*, 2008). Despite clear detection of various CK metabolites in xylem sap in various plant species (reviewed in Hirose *et al.*, 2008), we did not observe any immuno-signal in xylem vessels in the pedicel (Fig. 2). Presumably this is because these dead cells are devoid of specific cellular proteins

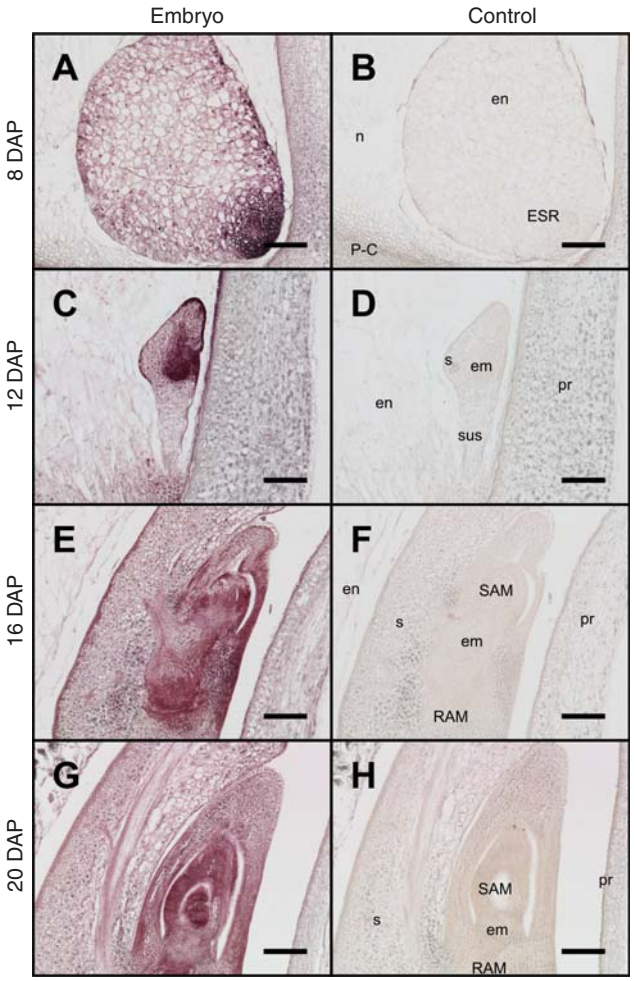

FIG. 4. CK immunolocalization on the central longitudinal section of caryopsis showing developing embryo between 8 and 20 DAP. The visible area of the panels is represented in the schematic caryopsis drawing of Fig. 1. Abbreviations: em, embryo; en, endosperm; ESR, embryo-surrounding region; n, nucellus; P-C, placento-chalaza; pr, pericarp; RAM, root apical meristem; SAM, shoot apical meristem; s, scutellum; sus, suspensor. Scale bars = 100 μm.

that provide binding sites for CK ribosides and glucosides, which normally react with the primary antibody in the immunoassays (Sossountzov *et al.*, 1988; Dewitte *et al.*, 1999).

Another significant observation here is a rapid and large increase in the CK levels observed only in the fertilized caryopses; unfertilized ovules of the same age showed only basal levels that were less than one-tenth of the former (Figs 2 and 5). Importantly, the high levels of CK in the pedicel at 6–8 DAP were coincident with a significant level of DNA synthesis in the coenocytic phase and/or transition to a cellular phase of development in filial tissue (Kowles and Phillips, 1985). Clearly, signalling for CK transportation and/or *de novo* (local) biosynthesis in the pedicel originated in the filial tissues. Evidence for the local biosynthesis in the pedicel at 7 and 14 DAP is available through *in situ* hybridization for the CK biosynthetic *ZmIPT1* gene (Fig. 6). Similar results regarding the expression of two *ZmIPT* genes in the pedicel have also been reported recently (Vyroubalová *et al.*, 2009); however, these studies do not provide critical data on cellular specificity and/or developmental stage specificity of the material analysed.

Both high levels and high diversity in the CK forms in the pedicel raise an important question regarding their possible roles in addition to their participation in cell divisions in the filial tissues. Photosynthate and nutrients are uploaded into the pedicel through vascular elements prior to entry into the basal endosperm cells and subsequent mobilization into the upper parts of the endosperm and embryo. In response to the growth, development and sink strength of the filial tissue, the pedicel also undergoes significant growth and differentiation, including a major phase of developmental PCD (Kladnik *et al.*, 2004). Our previous studies have shown that fertilization-dependent PCD in the P-C layers is a non-cell-autonomous phenomenon that leads to many layers of empty cells just beneath the BETL. We suggest that the high levels of CKs in the pedicel may be causal to the occurrence of developmental PCD in the P-C layers. Our hypothesis is prompted by the significant spatial and temporal coincidence between PCD and the high CK levels; indeed, we did not

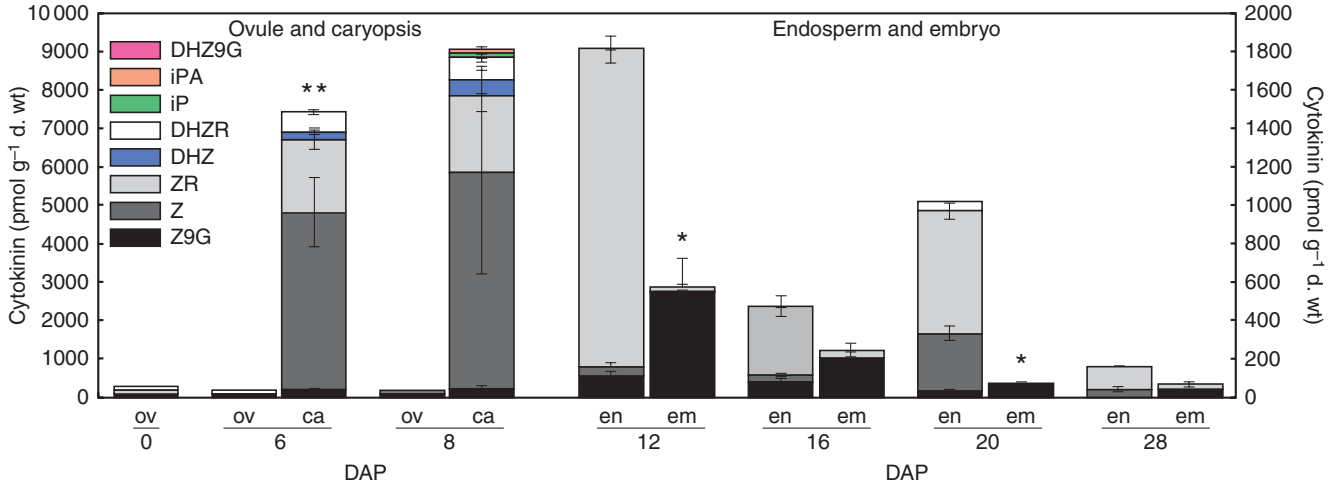

FIG. 5. CK content (pmol CK g^{-1} d. wt) in unpollinated ovules, developing endosperm and embryo from 0 to 28 DAP. Data represent the mean ± s.e. of three independent extractions. Asterisks indicate significant differences between endosperm and embryo at each developmental stage: $*P < 0{\cdot}05$, $**P < 0{\cdot}01$.

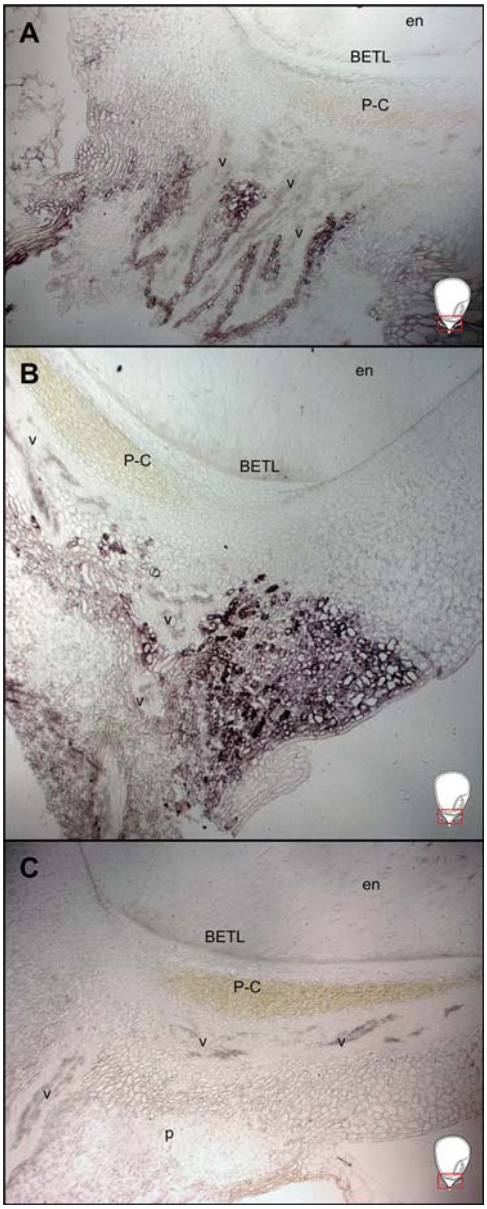

FIG. 6. *In situ* hybridization of the *ZmIPT1* gene transcript on the pedicel region of the central longitudinal sections of developing caryopsis at 7 and 14 DAP: (A) 7 DAP; (B) 14 DAP; (C) control reaction with the antisense probe. The visible area is represented by the rectangles in the schematic caryopsis drawings. Abbreviations: BETL, basal endosperm transfer layer; en, endosperm; p, pedicel; P-C, placento-chalaza; v, vascular tissue.

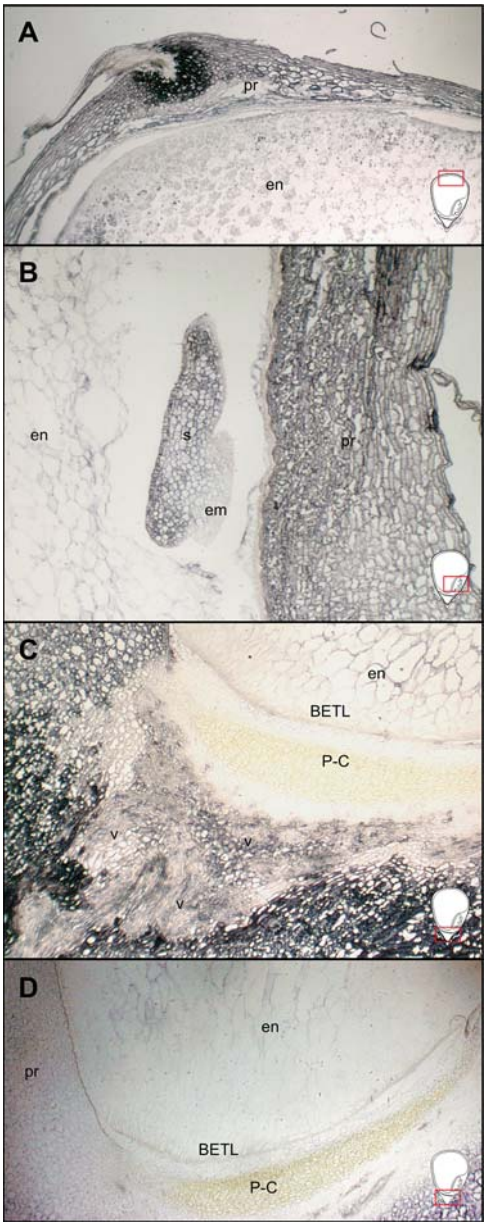

FIG. 7. *In situ* hybridization of the *ZmCNGT* gene transcript on the central longitudinal sections of developing caryopsis at 11 DAP. (A) Upper part of caryopsis; (B) close-up of embryo region; (C) basal endosperm, P-C layer and pedicel; (D) control reaction with the antisense probe. The visible area is represented by the red rectangles in the schematic caryopsis drawings. Abbreviations: BETL, basal endosperm transfer layer; em, embryo; en, endosperm; pr, pericarp; P-C, placento-chalaza; s, scutellum; v, vascular tissue.

immunolocalize any CK signal in the P-C layers themselves presumably because, similar to the xylem vessels, these cells were devoid of CK-binding proteins. Additionally, there is a large body of evidence from various cell culture studies that high concentrations of various CKs, including kinetin, benzylaminopurine (BA), iP, iPA and Z, lead to typical morphological and biochemical hallmarks of PCD (Mlejnek and Procházka, 2002; Mlejnek *et al.*, 2003; Bolduc *et al.*, 2007; Suda *et al.*, 2009). Induction of apoptotic PCD by BA has also been demonstrated in carrots and *Arabidopsis* cell cultures (Carimi *et al.*, 2003, 2004, 2005). Similar data from whole plants are lacking, except that injections of micromolar concentrations of BA at 0 DAP in maize resulted in significant loss of caryopsis weight and number; infusions at later stages did not show any detectable effect (Dietrich *et al.*, 1995). Whether such losses in seed number and mass are due to PCD is not known.

CKs in the filial tissues

At 8 DAP, the immuno-signal for CKs was detectable in the BETL region (Fig. 2). This is in agreement with data from

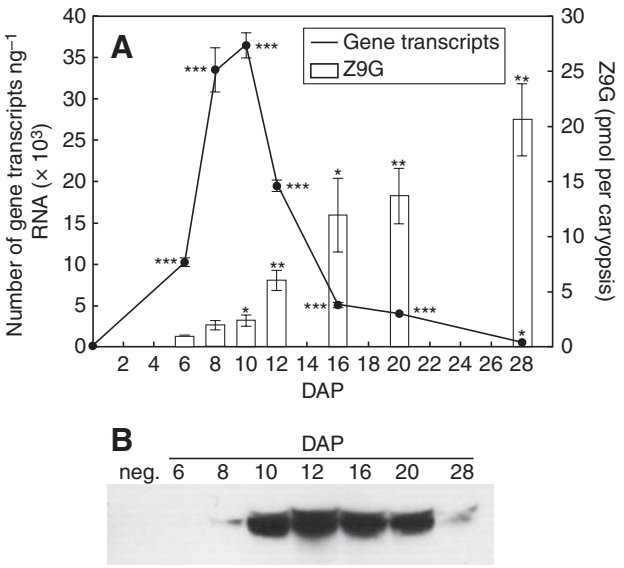

FIG. 8. Quantitative analysis of *ZmCNGT* transcript abundance and the amount of Z9G in caryopsis from 0 to 28 DAP (A) and immunoblotting analysis of ZmCNGT protein from 6 to 28 DAP; 50 μg of protein was loaded per lane (B). Values in (A) represent the mean ± s.e. of nine reactions for quantification of transcript, and of three independent cytokinin extractions for Z9G quantification. Asterisks indicate significant differences between the transcript or Z9G abundance at 0 DAP and other time points: $*P < 0{\cdot}05$, $**P < 0{\cdot}01$, $***P < 0{\cdot}001$.

Brugière *et al.* (2008) showing *in situ* hybridization in the BETL for the transcripts of the *ZmIPT2* gene encoding a critical enzyme of CK biosynthesis essential at the onset of mitosis in the endosperm. The relatively strong CK signal that was also seen throughout the endosperm from 8 to 12 DAP is probably associated with the proposed role of endosperm CKs in promoting cell divisions in this tissue (Dietrich *et al.*, 1995; Brugière *et al.*, 2008). Another prominent feature at 8 DAP was the clear delineation of the ESR from the rest of the endosperm by a very strong cytokinin signal (Fig. 2). The ESR lines the cavity of the endosperm in which the embryo develops. Its exact role is unknown but possible functions include a role in embryo nutrition, the establishment of a physical barrier between the embryo and the endosperm during seed development, and providing a zone for communication between the embryo and the endosperm (Olsen, 2004).

After 12 DAP most of the endosperm CK immuno-signal was localized to the outer layers of the endosperm, particularly the aleurone (Fig. 3). The labelling overlapped with the cessation of cell divisions in the central endosperm and their continuation in the peripheral cell layers, away from the embryo until late developmental stages (Vilhar *et al.*, 2002; Rijavec *et al.*, 2009).

The CK concentration in the developing embryo was very low (Fig. 5) and it is not known to what extent and in which form the embryo CKs are transported from the surrounding endosperm or are synthesized by *ZmIPT1*, *ZmIPT2*, *ZmIPT10* or other *IPT* genes expressed in the embryo (Vyroubalová *et al.*, 2009). The major moiety of all detected CKs in the embryo was Z9G (Fig. 5). Although the biochemical characteristics of a ZmCNGT protein involved in the 9-glucosylation has not been fully evaluated yet (Fig. 8), the bioinformatic analysis (Supplementary Data Figs S1 and S2) together with *in situ* localization of its gene transcript in pedicel, pericarp and scutellum (Fig. 7) provide us with insight into the process of CK inactivation. Strikingly, the spatial and temporal distribution of *ZmCNGT* and Z9G in these tissues matched the distribution of several CK dehydrogenase genes and corresponding proteins (Bilyeu *et al.*, 2003; Brugière *et al.*, 2003; Massonneau *et al.*, 2004; Šmehilová *et al.*, 2009; Vyroubalová *et al.*, 2009). This might indicate a putative synergistic role of CK degradation and *N*9-glucosylation during development. For instance, CK dehydrogenase might regulate CK levels entering an organ by controlling CK flux transiting the xylem via a feedback control mechanism (Brugière *et al.*, 2003). A recent report on the cellular localization and biochemical comparison of several CK dehydrogenases (Šmehilová *et al.*, 2009) may shed new light on the complementary function of different conjugate CK forms. Recombinant ZmCKX10 protein produced in *Pichia pastoris* very effectively degrades Z9G. *ZmCKX10* transcript has been demonstrated in relative high abundance both in maize pedicel and embryo (Šmehilová *et al.*, 2009; Vyroubalová *et al.*, 2009). However, a considerable amount of further work is necessary to determine the nature of *N*9-glucoside forms of CKs and how this class of proteins contributes to the complexity of CK homeostatic regulation in plants.

In conclusion, our correlative data suggest that CKs may perform highly contrasting roles in the filial endosperm and maternal tissues of a developing seed in maize. High levels of CK in the filial tissue coincided with an early phase of developmental known to be associated with DNA replication and cell division in the endosperm. In contrast, the similar high levels in the maternal pedicel region were associated with developmental PCD that led to complete loss of nuclei and membranous structures, and ultimately, the empty cells. Interestingly, signalling for the developmental PCD appeared to be triggered by metabolic events in the filial endosperm.

SUPPLEMENTARY DATA

Supplementary data are available online at www.aob.oxfordjournals.org and consist of the following figures. Fig. S1: Alignment of maize putative ZmCNGT protein with *Arabidopsis* and maize CNGTs. Fig. S2: Phylogenetic tree calculated using full-length *N*-glucosyl transferase proteins from *Arabidopsis*, *Phaseolus* and *Zea mays*.

ACKNOWLEDGEMENTS

We thank the Slovenian Research Agency (grant 1000-05-310055 to T.R.) and the USA–Slovenia Cooperation in Science and Technology (grant BI-US/06-07-031). This was a cooperative investigation by the US Department of Agriculture, Agricultural Research Service, and the Institute of Food and Agricultural Sciences, University of Florida. We gratefully acknowledge Q.-B. Li for technical assistance and Dr Aleš Kladnik for help with immunolocalization experiments. We thank Drs David Clark, B.-H. Kang and D. R. Pring for critical reading of the manuscript.

LITERATURE CITED

Bilyeu KD, Laskey JG, Morris RO. 2003. Dynamics of expression and distribution of CK oxidase/dehydrogenase in developing maize kernels. *Plant Growth Regulation* **39**: 195–203.

Bolduc N, Lamb NG, Cessna SG, Brisson LF. 2007. Modulation of Bax Inhibitor-1 and cytosolic Ca^{2+} by CKs in *Nicotiana tabacum* cells. *Biochimie* **89**: 961–971.

Brugière N, Jiao S, Hantke S, *et al*. 2003. CK oxidase gene expression in maize is localized to the vasculature, and is induced by CKs, abscisic acid, and abiotic stress. *Plant Physiology* **132**: 1228–1240.

Brugière N, Humbert S, Rizzo N, Bohn J, Habben JE. 2008. A member of the maize isopentenyl transferase gene family, *Zea mays* isopentenyl transferase 2 *ZmIPT2*, encodes a CK biosynthetic enzyme expressed during kernel development. *Plant Molecular Biology* **67**: 215–229.

Brzobohatý B, Moore I, Palme K. 1994. CK metabolism: implications for regulation of plant growth and development. *Plant Molecular Biology* **26**: 1483–1497.

Carimi F, Zottini M, Formentin E, Terzi M, Lo Schiavo F. 2003. CKs: new apoptotic inducers in plants. *Planta* **216**: 413–421.

Carimi F, Terzi M, De Michele R, Zottini M, Lo Schiavo F. 2004. High levels of the CK BAP induce PCD by accelerating senescence. *Plant Science* **166**: 963–969.

Carimi F, Zottini M, Costa A, Cattelan I, de Michelle R, Terzi M. 2005. NO signalling in CK-induced programmed cell death. *Plant, Cell & Environment* **28**: 1171–1178.

Chenna R, Sugawara H, Koike T, *et al*. 2003. Multiple sequence alignment with the Clustal series of programs. *Nucleic Acids Research* **31**: 3497–3500.

Dewitte W, Chiappetta A, Azmi A, *et al*. 1999. Dynamics of CKs in apical shoot meristems of a day-neutral tobacco during floral transition and flower formation. *Plant Physiology* **119**: 111–122.

Dietrich JT, Kaminek M, Blevins DG, Reinbott TM, Morris RO. 1995. Changes in CKs and CK oxidase activity in developing maize kernels and the effects of exogenous CK on kernel development. *Plant Physiology and Biochemistry* **33**: 327–336.

Emery N, Atkins C. 2006. CKs and seed development. In: Basra AS. ed. *Handbook of seed science and technology*. Binghamton, NY: The Haworth Press, 63–93.

Erlanger BF, Beiser SM. 1964. Antibodies specific for ribonucleosides and ribonucleotides and their reaction with DNA. *Proceedings of the National Academy of Sciences of the USA* **52**: 68–74.

Hirose N, Takei K, Kuroha T, Kamada-Nobusada T, Hayashi H, Sakakibara H. 2008. Regulation of cytokinin biosynthesis, compartmentalization and translocation. *Journal of Experimental Botany* **59**: 75–83.

Hou B, Lim EK, Higgins GS, Bowles DJ. 2004. N-glucosylation of CKs by glycosyltransferases of *Arabidopsis thaliana*. *The Journal of Biological Chemistry* **279**: 47822–47832.

Jackson DP. 1991. *In situ* hybridization in plants. In: Gurr SJ, McPherson M, Bowels DJ. eds. *Molecular plant pathology: a practical approach*. Oxford: Oxford University Press, 163–174.

Jones RJ, Schreiber BM, McNeil K, Brenner ML. 1990. Hormonal regulation of maize kernel development: the role of CKs. *Preceedings of the Plant Growth Regulator Society of America* **17**: 183–196.

Kang B-H, Xiong Y, Williams DS, Pozueta-Romero D, Chourey PS. 2009. Miniature1-encoded cell wall invertase is essential for assembly and function of wall-in-growth in the maize endosperm transfer cell. *Plant Physiology* **151**: 1366–1376.

Kladnik A, Chamusco K, Dermastia M, Chourey PS. 2004. Evidence of programmed cell death in post-phloem transport cells of the maternal pedicel tissue in developing caryopsis of maize. *Plant Physiology* **136**: 3572–3581.

Kowles RV, Phillips RL. 1985. DNA amplification patterns in maize endosperm nuclei during kernel development. *Proceedings of the National Academy of Sciences of the USA* **82**: 7010–7014.

LeClere S, Eric A, Schmelz EA, Chourey PS. 2007. Phenolic compounds accumulate specifically in maternally-derived tissues of developing maize kernels. *Cereal Chemistry* **84**: 350–356.

Lur HS, Setter TL. 1993. Endosperm development of maize defective-kernel dek. mutants – auxin and CK levels. *Annals of Botany* **72**: 1–6.

Martin RC, Mok MC, Habben JE, Mok DWS. 2001. A maize CK gene encoding an O-glucosyltransferase specific to *cis*-zeatin. *Proceedings of the National Academy of Sciences of the USA* **98**: 5922–5926.

Massonneau A, Houba-Herin N, Pethe C, *et al*. 2004. Maize CK oxidase genes: differential expression and cloning of two new cDNAs. *Journal of Experimental Botany* **55**: 2549–2557.

Mlejnek P, Procházka S. 2002. Activation of caspase-like proteases and induction of apoptosis by isopentenyladenosine in tobacco BY-2 cells. *Planta* **215**: 158–166.

Mlejnek P, Doležel P, Procházka S. 2003. Intracellular phosphorylation of benzyladenosine is related to apoptosis induction in tobacco BY-2 cells. *Plant, Cell & Environment* **26**: 1723–1735.

Morris RO. 1997. Hormonal regulation of seed development. In: Larkins BA, Vasil IK. eds. *Cellular and molecular biology of plant seed development*. Dordrecht: Kluwer, 117–149.

Olsen O-A. 2004. Nuclear endosperm development in cereals and *Arabidopsis thaliana*. *The Plant Cell* **16**: S214–S227.

Rijavec T, Kovač M, Kladnik A, Chourey PS, Dermastia M. 2009. A comparative study on the role of CKs in caryopsis development in the maize miniature1 seed mutant and its wild type. *Journal of Integrative Plant Biology* **51**: 840–849.

Rodó AP, Brugière N, Vankova R, *et al*. 2008. Over-expression of a zeatin O-glucosylation gene in maize leads to growth retardation and tasselseed formation. *Journal of Experimental Botany* **59**: 2673–2686.

Sambrook J, Fritsch EF, Maniatis T. 1989. *Molecular cloning: a laboratory manual*, 2nd edn. Cold Spring Harbor: Cold Spring Harbor Laboratory Press.

Sossountzov L, Maddiney R, Sotta B, *et al*. 1988. Immunocytochemical localization of CKs in *Craigella tomato* and a sideshootless mutant. *Planta* **175**: 291–304.

Suda N, Iwai H, Satoh S, Sakai S. 2009. Benzyladenine arrests cell cycle progression in G1 phase in tobacco BY-2 cells preceding induction of cell death. *Plant Biotechnology* **26**: 225–235.

Šmehilová M, Galuszka P, Bilyeu KD, *et al*. 2009. Subcellular localization and biochemical comparison of cytosolic and secreted CK dehydrogenase enzymes from maize. *Journal of Experimental Botany* **60**: 2701–2712.

Veach YK, Martin RC, Mok DWS, Malbeck J, Vankova R, Mok MC. 2003. O-glucosylation of *cis*-zeatin in maize. Characterization of genes, enzymes, and endogenous CKs. *Plant Physiology* **131**: 1374–1380.

Vilhar B, Kladnik A, Blejec A, Chourey PS, Dermastia M. 2002. Cytometrical evidence that the loss of seed weight in the *miniature1* seed mutant of maize is associated with reduced mitotic activity in the developing endosperm. *Plant Physiology* **129**: 23–30.

Vyroubalová Š, Václavíková K, Turecková V, *et al*. 2009. Characterization of new maize genes putatively involved in CK metabolism and their expression during osmotic stress in relation to CK levels. *Plant Physiology* **151**: 433–447.

Whelan JA, Russell NB, Whelan MA. 2003. A method for the absolute quantification of cDNA using real-time PCR. *Journal of Immunological Methods* **278**: 261–269.